

D-mesons propagation in hadronic matter and consequences on heavy-flavor observables in ultrarelativistic heavy-ion collisions

V. Ozvenchuk,* J. M. Torres-Rincon, P. B. Gossiaux, and J. Aichelin
Subatech, UMR 6457, IN2P3/CNRS, Université de Nantes,
École des Mines de Nantes, 4 rue Alfred Kastler, 44307 Nantes cedex 3, France

L. Tolos
Institut de Ciències de l'Espai (IEEC/CSIC), Campus Universitat Autònoma de Barcelona,
Facultat de Ciències, Torre C5, E-08193 Bellaterra, Spain and
Frankfurt Institute for Advanced Studies, Johann Wolfgang Goethe-Universität,
Ruth-Moufang-Str. 1, 60438 Frankfurt am Main, Germany
(Dated: March 25, 2019)

We employ recently published cross sections for *D*-mesons with hadrons and calculate the drag and diffusion coefficients of *D*-mesons in hadronic matter as a function of the momentum of *D*-mesons as well as of the temperature of the medium. Calculating in our approach the spatial diffusion coefficient, D_x , at zero chemical potential we see a very smooth transition between our calculations for the hadron gas and the lattice QCD calculations. Applying the results for the transport coefficients of *D*-mesons in a Fokker-Planck equation, which describes the evolution of *D*-mesons during the expansion of a hadron gas created in ultrarelativistic heavy-ion collisions, we find that the value of R_{AA} is little influenced by hadronic rescattering, whereas in the elliptic flow the effects are stronger. We extend our calculations to the finite chemical potentials and calculate the spatial diffusion coefficients of *D*-mesons propagating through the hadronic medium following isentropic trajectories, appropriate at future FAIR and NICA heavy-ion experiments. For the isentropic trajectory with $s/\rho_B^{\text{net}} = 20$ we find a perfect matching of results for *D*-mesons in hadronic matter and for charm quarks in partonic matter treated within the DQPM approach.

I. INTRODUCTION

A new state of matter, a deconfined phase of quarks and gluons known as quark-gluon plasma (QGP), has been created in ultrarelativistic heavy-ion collisions at the Relativistic Heavy-Ion Collider (RHIC) at Brookhaven National Laboratory (BNL) [1–4] and at the Large Hadron Collider (LHC) at the European Organization for Nuclear Research (CERN) [5].

Heavy-flavor (HF) particles have been suggested to study the properties of the QGP. Heavy quarks (charm and bottom) are produced in the initial hard nucleon-nucleon scatterings and their initial momentum distribution can be directly inferred from proton-proton collisions. Initially the heavy quarks have no elliptic flow. Their thermal equilibration time is larger than the QGP lifetime in heavy-ion collisions (HICs). Thus the interaction between heavy quarks and the partons of the QGP modify the heavy quark spectra but do not bring heavy quarks to a thermal equilibrium.

A direct measure of the interaction of the heavy quarks with the QGP medium created in HICs is the nuclear modification factor, R_{AA} , which is the ratio of the p_T distribution measured in HICs and the reference p_T distribution from proton-proton collisions scaled by the number of binary collisions. It is therefore one if a HIC is just an ensemble of independent pp collisions. The

R_{AA} of intermediate- and high- p_T HF mesons and single nonphotonic electrons originating from the decays of HF mesons, experimentally measured at RHIC [6–8] and LHC [10, 11], is significantly below unity. It indicates a substantial energy loss of high- p_T heavy quarks in the QGP. The observed finite elliptic flow, v_2 , of HF mesons and decay electrons [6, 9, 11, 12] is either due to the interactions with light quarks and gluons in the plasma leading to the partial thermalization of low- and intermediate- p_T heavy quarks or due to the coalescence at the end of the deconfined phase.

The large masses of charm (c) and bottom (b) motivated different authors to calculate the time evolution of distribution function of heavy quarks in a plasma by a Fokker-Planck (FP) equation [13–23]. In such an approach the drag and diffusion coefficients depend on the temperature of the expanding plasma and the momentum of the heavy quark. The instantaneous temperature of the expanding plasma is an input in these calculations. It may be obtained by a hydrodynamical description of the expanding plasma. Later it turned out that the small scattering angle assumption, inherent in a FP approach, is not completely justified and therefore approaches have been launched which replace the FP equation by a Boltzmann equation [24, 25].

In order to exploit the HF particles as an efficient probe for the understanding of the time evolution of the partonic matter the effects of the interactions of HF hadrons with hadronic matter has to be understood and the observables have to be corrected for this effect. Different approaches have been used to study the interaction of

*Electronic address: Vitalii.Ozvenchuk@subatech.in2p3.fr

HF mesons in hadronic matter [26–34]. This interaction has been usually described in form of drag and diffusion coefficients. The diffusion coefficient of D -mesons was calculated using an effective theory incorporating both chiral and heavy-quark symmetries [26]. In Ref. [27] the drag and diffusion coefficients of D -mesons were obtained employing empirical elastic scattering amplitudes of D -mesons with thermal hadrons. The interactions of D -mesons with light mesons and baryons were evaluated using Born amplitudes [28] and within an unitarized approach based on effective models [31].

In the present paper, we calculate the drag and diffusion coefficients of D -mesons propagating in hadronic matter by extending the model of Ref. [31]. Subsequently we implement the transport coefficients into our transport model [24, 25, 35]. This model was developed to describe the momentum distribution of heavy quarks or HF mesons produced in HICs, and to evaluate the nuclear modification factor and elliptic flow of D -mesons as well as of single nonphotonic electrons originating from the decays of HF mesons in HICs at $\sqrt{s} = 200$ GeV at RHIC. Finally, we extend our calculations and present the D -meson propagation in hadronic medium following isentropic trajectories, appropriate at future FAIR and NICA heavy-ion experiments.

The paper is organized as follows. In Sec. II we provide the detailed description of the model, which is used to propagate heavy quarks and HF mesons in the bulk medium. We discuss in Sec. III the hadronic cocktail used to calculate the D -meson drag and diffusions coefficients. In Sec. IV we then present the results for the transport coefficients of D -mesons and compare these results to previous studies in this topic. The resulting nuclear modification factor, R_{AA} , and elliptic flow, v_2 , of D -mesons with the presence of D -meson rescattering in the hadronic medium are given in Sec. V. In Sec. VI we show the transport coefficients of D -meson at FAIR energies and Sec. VII is dedicated to the summary and outlook.

II. THE MODEL

In this study we use the Monte Carlo propagation of heavy quarks and HF mesons [24, 25, 35], MC@sHQ, within a 2+1d fluid dynamically expanding ideal plasma with smooth initial conditions and an equation of state with a first-order phase transition [36].

We initialize the heavy quarks at the original nucleon-nucleon scattering points according to the p_T -distribution from perturbative QCD (pQCD) results in fixed order plus next to leading logarithm (FONLL) [37–39]. They are isotropically distributed in the azimuthal direction and therefore v_2 is initially zero. In coordinate space the initial distribution of heavy quarks is given by the Glauber calculation.

The local temperature and velocity field determine the interactions of heavy quarks with locally thermalized par-

tons in the plasma. They allow us to evaluate the number density and momentum distribution of the plasma particles. Heavy quarks interact with plasma partons by either elastic or radiative collisions. The evolution of heavy quarks is described by the Boltzmann equation, which is solved by the test particle method, applying Monte Carlo techniques.

The elastic cross sections of heavy quarks with the gluons and light quarks in the plasma are obtained from pQCD matrix elements in Born approximation [13, 40] including an effective running coupling constant $\alpha_{\text{eff}}(Q^2)$ [41–43], determined from electron-positron annihilation [44] as well as nonstrange hadronic decays of τ leptons [45]. For the gluon propagator we respectively use a hard thermal loop (HTL) approach [46, 47] and a semi-hard propagator [24] for small and large transferred momentum.

The hadronization of heavy quarks occurs when the energy density of the fluid cell is less than a critical value, $\varepsilon_c = 0.45$ GeV/fm³, (corresponding to a critical temperature of $T_c = 165$ MeV). There is a mixed phase (from $\varepsilon_{\text{max}} = 1.65$ GeV/fm³ to $\varepsilon_c = 0.45$ GeV/fm³) in our model at T_c , where all interaction rates are rescaled by a factor of $\varepsilon/\varepsilon_{\text{max}}$. The heavy quarks form hadrons via coalescence [25], predominantly for low- p_T heavy quarks, or fragmentation [48], predominantly for intermediate- and high- p_T quarks.

Originally it has been assumed in this model that after the hadronization HF mesons do not interact [24, 25]. This leads to some tension between the R_{AA} and the v_2 . It is one of the purposes of this article to study explicitly the interaction of D -mesons with hadrons in the medium consisting of light and strange mesons as well as of baryons and antibaryons (as described in Sec. III) and to see whether one can obtain a better agreement for R_{AA} and v_2 simultaneously. For this purpose we evaluate the drag and diffusion coefficients and use the FP equation (8) to calculate the modification of the spectrum as well as of the elliptic flow due to hadronic interactions. The hadronic medium during the expansion is described by [36].

III. THE HADRON GAS

In this section we concentrate on the description of the hadronic medium employed to evaluate the drag and diffusion coefficients of D -mesons propagating through a hadronic medium. In ultrarelativistic HICs at RHIC energies the chemical freeze-out of hadron ratios at a temperature of $T_{\text{ch}} \simeq 170$ MeV is significantly earlier than thermal freeze-out of the light hadrons at $T_{\text{th}} \simeq 90$ MeV. Thus, in a thermodynamical description of the cooling process from chemical to thermal freeze-out, the conservation of the observed particle ratios (given at the chemical freeze-out) can be achieved by the introduction of effective chemical potentials for all hadron species that are not subject to strong decays on the scale of the typical

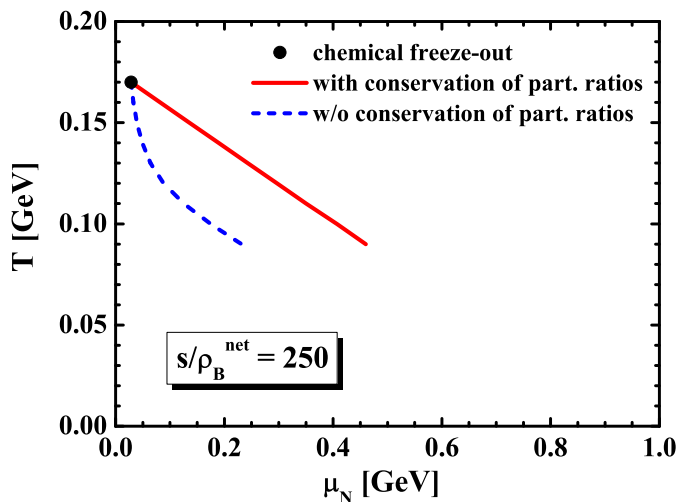


FIG. 1: Isentropic thermodynamic trajectories at top RHIC energies. Solid line includes the conservation of particle ratios and dashed line does not.

expansion time [49].

We simulate the hadron medium, which consists of light mesons (π , η , ρ , ω , η' , f_0 , a_0 , ϕ , h_1 , b_1 , a_1 , f_2 , f_1), strange mesons (K , K^* , K_1), nucleons (p , n), nuclear resonances [$N(1440)$, $N(1520)$, $N(1535)$, $N(1650)$, $N(1675)$, $N(1680)$, $N(1700)$] and Δ -resonances [$\Delta(1232)$, $\Delta(1600)$, $\Delta(1620)$, $\Delta(1700)$] as well as the corresponding antibaryons, at various values for the temperature [in a range from thermal (90 MeV) to chemical (170 MeV) freeze-out]. The study of thermal and chemical equilibration of a hadron matter in HICs have been performed in Ref. [50] using a transport model. If we implement the effective chemical potentials into the thermal hadron distribution functions the particle densities in the system at given temperature can be calculated as

$$n_i = d_i \int \frac{d^3k}{(2\pi)^3} \frac{1}{e^{[E_i - \mu_i(T)]/T} \pm 1}, \quad (i = \pi, K, \dots, N, \Delta) \quad (1)$$

and the total energy density is given by

$$\varepsilon = \sum_i d_i \int \frac{d^3k}{(2\pi)^3} \frac{E_i}{e^{[E_i - \mu_i(T)]/T} \pm 1}, \quad E_i = \sqrt{k^2 + m_i^2}, \quad (2)$$

where T denotes the temperature of the system, μ_i and d_i stand for the effective chemical potential and degeneracy factor of i -particle, respectively. In Eqs. (1, 2) upper (lower) signs refer to bosons (fermions), respectively.

We assume an adiabatic expansion with a specific entropy (i.e., entropy per net baryon) of $S/N_B^{\text{net}} = 250$ which is a characteristic value for collisions at the top RHIC energy. This entropy together with the temperature of chemical freeze-out, $T_{\text{ch}} = 170$ MeV, results in a baryon chemical potential of $\mu_B^{\text{ch}} = 28.3$ MeV. At chemical freeze-out temperature, T_{ch} , all meson effective chemical potentials are equal to zero, $\mu_m^{\text{ch}} = 0$. Starting from

the chemical freeze-out point and employing the entropy density

$$s = \mp \sum_i d_i \int \frac{d^3k}{(2\pi)^3} [\pm f \ln f + (1 \mp f) \ln(1 \mp f)], \quad (3)$$

as well as the net baryon density

$$\rho_B^{\text{net}} = \sum_{B_i} d_{B_i} \int \frac{d^3k}{(2\pi)^3} [f^{B_i}(\mu_{B_i}, T) - f^{\bar{B}_i}(\mu_{\bar{B}_i}, T)] \quad (4)$$

we can construct a thermodynamic trajectory in the μ_N - T plane for fixed $s/\rho_B^{\text{net}}(T) = 250$. The upper (lower) signs refer to fermions (bosons) and f are the particle thermal distribution functions. The sum is taken over all particles and over all baryons in Eqs. (3) and (4), respectively. The resulting trajectory is shown by the dashed line in Fig. 1. Note that, in this case all meson effective chemical potentials are equal to zero during the evolution, $\mu_m^{\text{eff}}(T) = 0$, i.e., we do not conserve the particle ratios during the expanding of the fireball from chemical to thermal freeze-out.

We come now to the expansion of the hadron gas in which the particle ratios are conserved. The effective pion number is defined as

$$N_\pi^{\text{eff}} = V \sum_i N_\pi^{(i)} n_i(T, \mu_i), \quad (5)$$

where V denotes the volume and n_i stands for the particle density of i -resonance with lifetimes shorter than the typical fireball lifetime. The effective pion number $N_\pi^{(i)}$ of a given resonance is determined by the number of pions in its decay modes taking into account the branching ratios, e.g., $N_\pi^{(\rho)} = N_\pi^{(f_0)} = 2$, $N_\pi^{(\Delta)} = N_\pi^{(K^*)} = 1$, $N_\pi^{(N(1440))} = 0.65 \cdot 1 + 0.35 \cdot 2 = 1.35$, etc. The corresponding effective chemical potentials for those resonances are defined with the same weighting, e.g., $\mu_\rho = \mu_{f_0} = 2\mu_\pi$, $\mu_\Delta = \mu_N + \mu_\pi$, $\mu_{K^*} = \mu_K + \mu_\pi$, $\mu_{N(1440)} = \mu_N + 1.35\mu_\pi$, etc. In analogy, all other effective meson numbers, which have to be conserved, can be defined for all mesons that are not subject to strong decays, e.g., for K , η , η' , ω , ϕ mesons. In our calculation we neglect the in-medium modifications of the spectral function of ω and ϕ mesons. As first pointed out by Rapp in Ref. [49], the explicit conservation of the number of antibaryons significantly affects the composition of the hadronic expansion at RHIC. This idea was then employed in the hadronic equation of state for the hydrodynamical model of Heinz and Kolb [51], which we use to describe the bulk medium in the MC@sHQ model. Thus, for the consistency of our calculations, we also conserve the number of antibaryons by introducing the effective antibaryon chemical potential, μ_B^{eff} , e.g., $\mu_{\bar{N}} = -\mu_N + \mu_B^{\text{eff}}$, $\mu_{\bar{\Delta}} = -\mu_\Delta + \mu_B^{\text{eff}} + \mu_\pi$. Now starting again from the freeze-out point we can construct an isentropic trajectory, $s/\rho_B^{\text{net}}(T) = 250$, keeping also the ratios of effective stable particle numbers to ef-

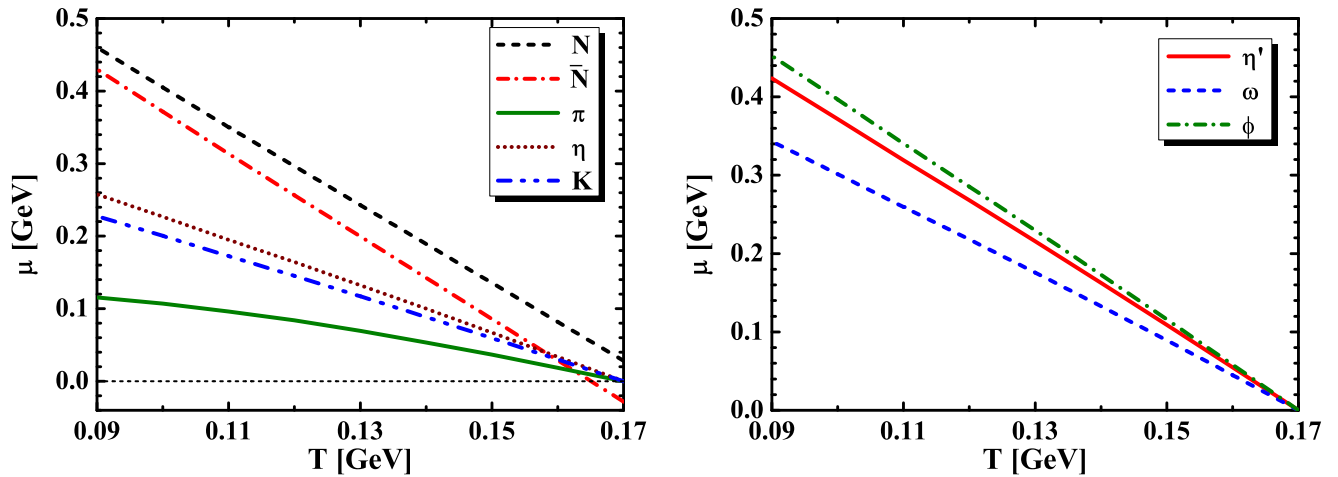


FIG. 2: The temperature dependence of effective chemical potentials for an isentropic hadronic fireball expansion at top RHIC energy for different particle species: (left panel) π (solid), N (dashed), \bar{N} (dash-dotted), η (dotted), K (dash-dot-dotted); (right panel) η' (solid), ω (dashed), ϕ (dash-dotted).

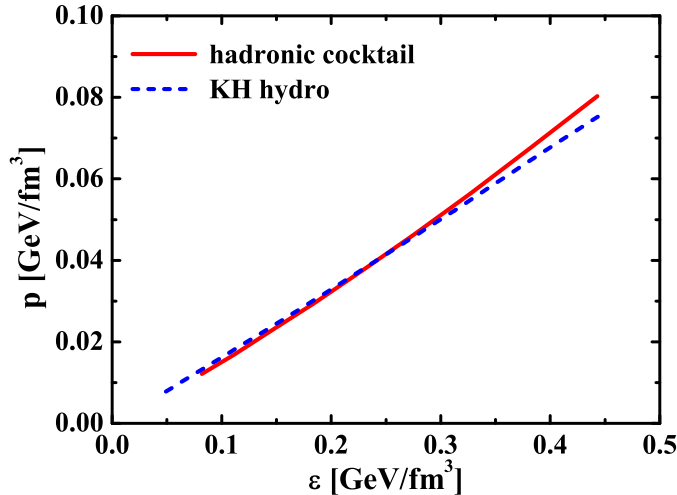


FIG. 3: The pressure as a function of energy density calculated in our approach (solid) in comparison to the result obtained from the hydrodynamical model [36] (dashed).

effective antibaryon number

$$\frac{N_B^{\text{eff}}}{N_B^{\text{eff}}}, \frac{N_\pi^{\text{eff}}}{N_B^{\text{eff}}}, \frac{N_\eta^{\text{eff}}}{N_B^{\text{eff}}}, \frac{N_K^{\text{eff}}}{N_B^{\text{eff}}}, \frac{N_\omega^{\text{eff}}}{N_B^{\text{eff}}}, \frac{N_{\eta'}^{\text{eff}}}{N_B^{\text{eff}}}, \frac{N_\phi^{\text{eff}}}{N_B^{\text{eff}}}, \quad (6)$$

fixed in the hadronic evolution toward thermal freeze-out. The resulting thermodynamic trajectory with the conservation of particle ratios is presented in Fig. 1 by the solid line. A fixed specific entropy density together with the conservation of particle ratios during the fireball evolution lead to an approximately linear increase of the effective meson chemical potentials with decreasing temperature, which are shown in Fig. 2 along with nucleon and antinucleon chemical potentials.

Before we proceed to the results for D -meson trans-

port coefficients the applicability of the results to the bulk medium in the MC@sHQ model has to be checked. Thus, we compare the equation of state used in our calculations to the hadronic equation of state employed in the hydrodynamical model of Heinz and Kolb [36]. The pressure in our hadronic cocktail can be calculated as

$$p = \sum_i d_i \int \frac{d^3k}{(2\pi)^3} \frac{k^2}{3E_i} \frac{1}{e^{[E_i - \mu_i(T)]/T} \pm 1}, \quad (7)$$

where the sum is taken over all particles in the system. We present in Fig. 3 the pressure (7) as a function of energy density (2) in comparison to the result from the hydrodynamical model [36]. After the examination of Fig. 3 we can conclude that the equations of state are in agreement.

IV. THE D -MESON TRANSPORT COEFFICIENTS

The propagation of D -mesons in the hadronic medium is evaluated using the FP equation

$$\frac{\partial f(\mathbf{p}, t)}{\partial t} = \frac{\partial}{\partial p_i} \left[A_i(\mathbf{p}) f(\mathbf{p}, t) + \frac{\partial}{\partial p_j} B_{ij}(\mathbf{p}) f(\mathbf{p}, t) \right], \quad (8)$$

which describes the time evolution of the distribution of the heavy quark $f(\mathbf{p}, t)$ in a medium characterized by the (time dependent) drag, $A_i(\mathbf{p})$, and diffusion, $B_{ij}(\mathbf{p})$, coefficients, which are given by

$$A_i(\mathbf{p}) = \int d\mathbf{k} \omega(\mathbf{p}, \mathbf{k}) k_i, \quad (9)$$

$$B_{ij}(\mathbf{p}) = \int d\mathbf{k} \omega(\mathbf{p}, \mathbf{k}) k_i k_j. \quad (10)$$

$\omega(\mathbf{p}, \mathbf{k})$ is the transition rate for a collisions of a D -meson with heat-bath particles with initial \mathbf{p} and final $\mathbf{p} - \mathbf{k}$ momenta, \mathbf{k} being the transferred momentum. For the elastic scattering of a D -meson with momentum \mathbf{p} on a thermal hadron with momentum \mathbf{q} , the transition rate, $\omega(\mathbf{p}, \mathbf{k})$, can be expressed as

$$\omega(\mathbf{p}, \mathbf{k}) = g_h \int \frac{d\mathbf{q}}{(2\pi)^3} f_h(\mathbf{q}) v_{\text{rel}} \frac{d\sigma}{d\Omega}(\mathbf{p}, \mathbf{q} \rightarrow \mathbf{k}, \mathbf{q} + \mathbf{k}). \quad (11)$$

Here the index h stands for the hadrons in the thermal bath, g_h represents the spin-isospin degeneracy factor and f_h is the Bose or Fermi distribution for thermal hadrons. The relative velocity, v_{rel} , is determined as

$$v_{\text{rel}} = \frac{\sqrt{(p \cdot q)^2 - (m_D m_h)^2}}{E_D E_h}, \quad (12)$$

where $p = (E_D, \mathbf{p})$ and $q = (E_h, \mathbf{q})$ are the four-momenta of the D -meson and the thermal hadron, respectively.

For an isotropic background medium, the drag, $A_i(\mathbf{p})$, and diffusion, $B_{ij}(\mathbf{p})$, coefficients can be written as

$$A_i(\mathbf{p}) = \gamma(\mathbf{p}) p_i, \quad (13)$$

$$B_{ij}(\mathbf{p}) = B_0(\mathbf{p}) P_{ij}^\perp(\mathbf{p}) + B_1(\mathbf{p}) P_{ij}^\parallel(\mathbf{p}), \quad (14)$$

where the projection operators on the transverse and longitudinal momentum components are given by

$$P_{ij}^\perp(\mathbf{p}) = \delta_{ij} - \frac{p_i p_j}{\mathbf{p}^2}, \quad P_{ij}^\parallel(\mathbf{p}) = \frac{p_i p_j}{\mathbf{p}^2}. \quad (15)$$

Then the scalar coefficients can be represented as

$$\gamma(\mathbf{p}) = \int d\mathbf{k} \omega(\mathbf{p}, \mathbf{k}) \frac{k_i p_i}{\mathbf{p}^2}, \quad (16)$$

$$B_0(\mathbf{p}) = \frac{1}{4} \int d\mathbf{k} \omega(\mathbf{p}, \mathbf{k}) \left[\mathbf{k}^2 - \frac{(k_i p_i)^2}{\mathbf{p}^2} \right], \quad (17)$$

$$B_1(\mathbf{p}) = \frac{1}{2} \int d\mathbf{k} \omega(\mathbf{p}, \mathbf{k}) \frac{(k_i p_i)^2}{\mathbf{p}^2}, \quad (18)$$

where the dynamics enters through the transition rates.

In order to calculate the D -meson drag and diffusion coefficients in a hot hadron gas, which is discussed in Sec. III, we initialize the D -meson in the medium with different initial momenta \mathbf{p} at different temperatures. The initial transverse momentum of the D -meson is zero. We implement into the simulation the cross sections for the elastic scattering of a D -meson with hadrons as follows

1. For $D\pi \rightarrow D\pi$, $D\eta \rightarrow D\eta$, and $DK(\bar{K}) \rightarrow DK(\bar{K})$ elastic scattering processes the cross sections are taken from Ref. [31]; for $D\rho \rightarrow D\rho$ the cross section is taken from Ref. [52].

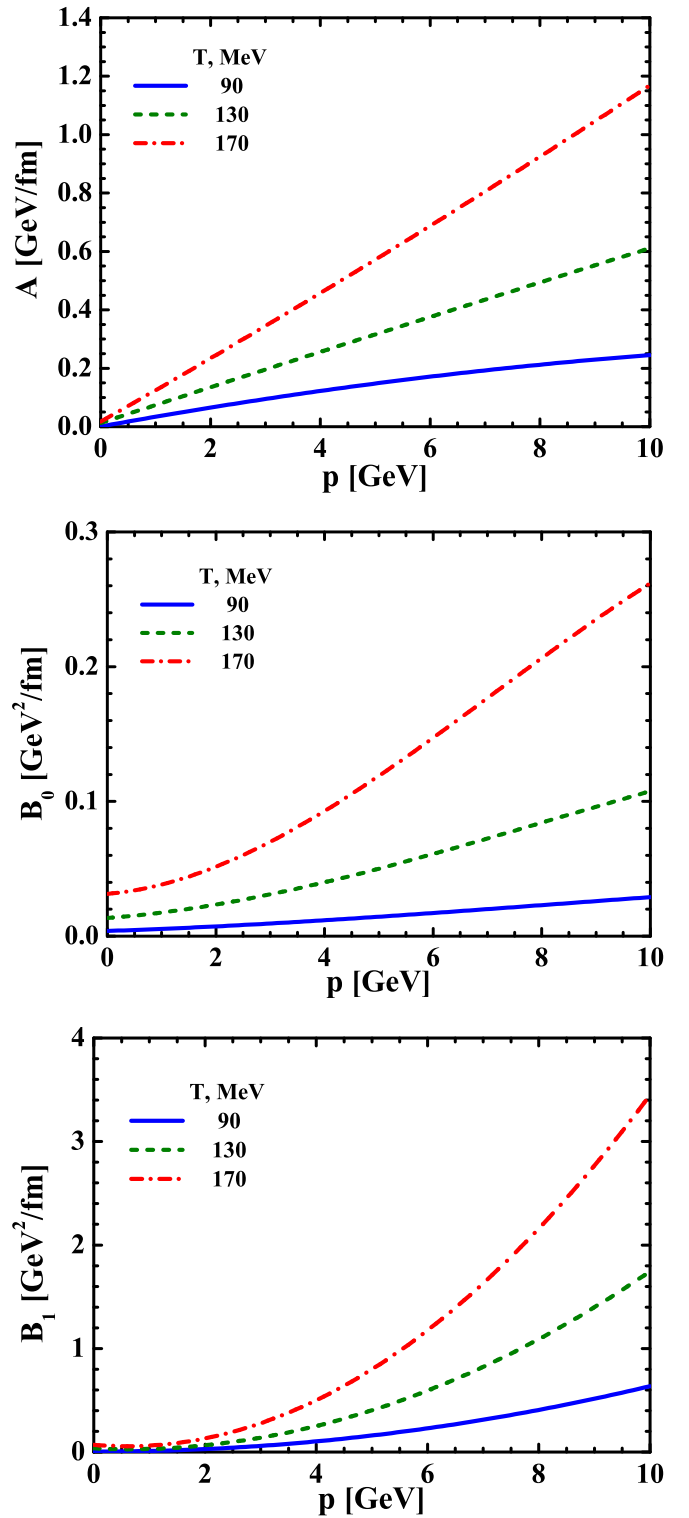


FIG. 4: The transport coefficients as a function of the initial momentum of the D -meson for systems at different temperatures: drag, A (upper panel); transverse diffusion, B_0 (middle panel); longitudinal diffusion, B_1 (lower panel).

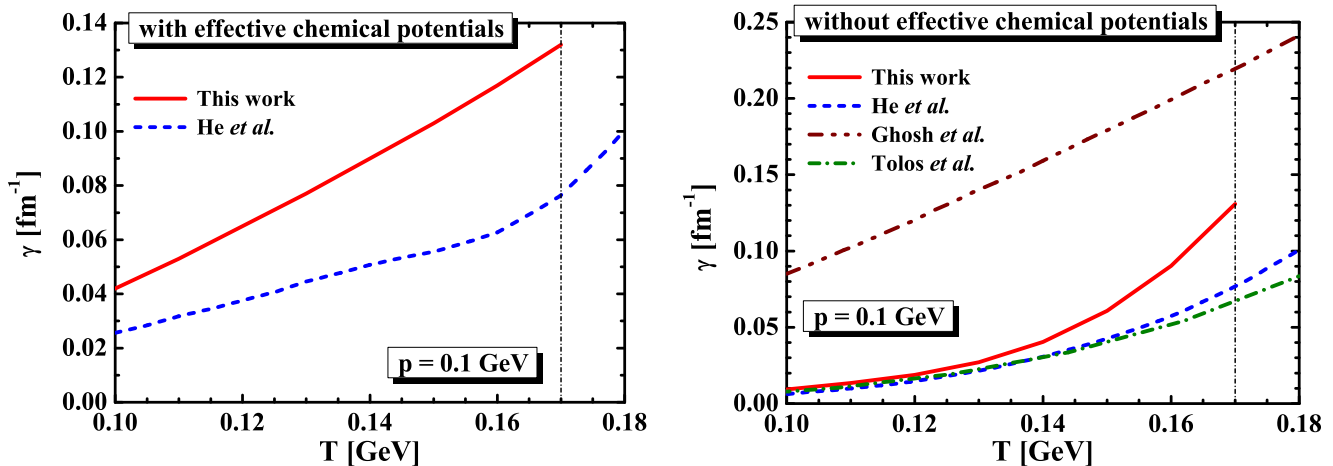


FIG. 5: The thermal relaxation rate of D -meson at momentum $p = 0.1$ GeV as a function of temperature with (left panel) and without (right panel) introducing effective chemical potentials to the hadronic cocktail. The solid lines represent our results, the model estimates from Ref. [27] are shown by the dashed lines, the dash-dot-dotted line depicts the result from Ref. [28] and the calculation from Ref. [31] is presented by the dash-dotted line.

2. For $Dm \rightarrow Dm$ elastic scattering processes, where m stands for a meson not listed above the cross sections are taken as constant, $\sigma = 10$ mb, following the calculation of M. He *et al.* [27].
3. For $DN(\bar{N}) \rightarrow DN(\bar{N})$ and $D\Delta(\bar{\Delta}) \rightarrow D\Delta(\bar{\Delta})$ elastic scattering processes, where $N = n, p$ and $\Delta = \Delta(1232)$, the cross sections are taken from Ref. [31].
4. For $DB \rightarrow DB$ and $D\bar{B} \rightarrow D\bar{B}$ elastic scattering processes, where $B(\bar{B})$ is baryon (antibaryon) not listed above the cross sections are taken as constant, $\sigma = 15$ mb, following the calculation of M. He *et al.* [27].

For different initial momenta of the D -meson we calculate the following average quantities:

$$\left\langle \frac{dp_z}{dt} \right\rangle, \left\langle \frac{dp_T^2}{dt} \right\rangle, \left\langle \frac{dp_z^2}{dt} \right\rangle - 2p_z \left\langle \frac{dp_z}{dt} \right\rangle, \quad (19)$$

which are related to the transport coefficients by

$$\begin{aligned} A &= A_z = -\left\langle \frac{dp_z}{dt} \right\rangle, \\ B_0 &= \frac{1}{4} \left\langle \frac{dp_T^2}{dt} \right\rangle, \\ B_1 &= \frac{1}{2} \left[\left\langle \frac{dp_z^2}{dt} \right\rangle - 2p_z \left\langle \frac{dp_z}{dt} \right\rangle \right]. \end{aligned} \quad (20)$$

We note that the drag coefficient A in Eq. (20) corresponds to $A_i(\mathbf{p})$ for $i = z$, which is given by Eq. (13).

In Fig. 4 we present the drag and diffusion coefficients as a function of the momentum of the D -meson propagating through a hadronic medium at different temperatures. We find that the transport coefficients increase

with the momentum of the D -meson and with the temperature of the medium. The dominant contributions to the drag and diffusion coefficients come from pions, but at higher temperatures the contributions from other (heavier) hadrons become important as well.

In addition, we evaluate the thermal relaxation rate of D -meson, which is defined by

$$\gamma = \lim_{p \rightarrow 0} \frac{A}{p}. \quad (21)$$

The results of our calculations as well as the comparison with other previous studies are shown in Fig. 5. The left panel of Fig. 5 presents the results obtained from our calculation (solid line) in comparison to the results of Ref. [27] (dashed line) in which as well effective chemical potentials have been introduced. The difference between those calculations at lower temperatures is due to the different cross sections for the D -meson scattering with the hadrons in the medium as well as due to slightly different effective chemical potentials in both models. At higher temperatures the difference is a consequence of the larger number of hadron species in our calculations, necessary to have a critical energy density of $\varepsilon_c = 0.45$ GeV/fm³ that increase the thermal relaxation rate of D -meson. The same differences one finds in the right panel of Fig. 5, where the calculations without effective chemical potentials are shown. In this calculation the pion/proton ratio increases with decreasing temperature so that at the end of the expansion the hadron gas consists of π 's only. The unphysical large value for the relaxation time obtained in Ref. [28] (dash-dot-dotted line) comes from the scattering amplitudes for the D -meson interactions with the thermal bath that rapidly grows with energy and breaks the unitarity condition for the S -matrix. In this work we use the same D -hadron cross sections as in Ref. [31] and the difference between the results at higher temperatures

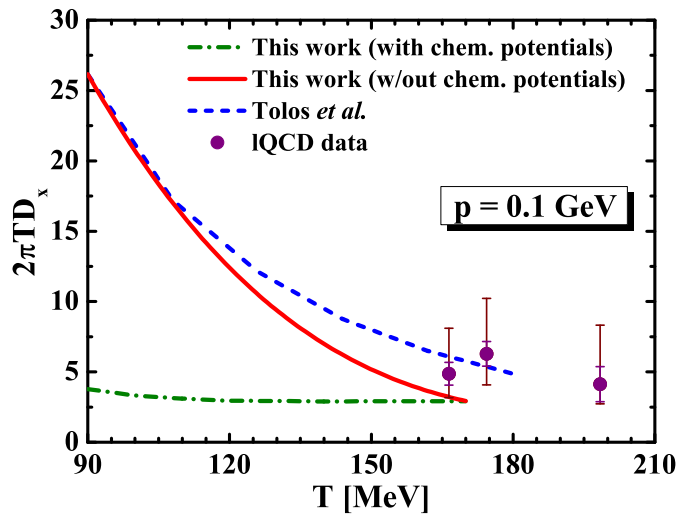


FIG. 6: The spatial diffusion coefficient of D -meson at momentum $p = 0.1$ GeV as a function of temperature with (dash-dotted line) and without (solid line) the introduction of effective chemical potentials to the hadronic cocktail in comparison to the results from Ref. [31] (dashed line). The IQCD data are taken from Ref. [53] (symbols).

is again due to the presence of the more states in our hadronic cocktail. When we employ the same hadronic cocktail (pions, kaons, etas, nucleons and Δ -baryons) as in Ref. [31], we reproduce their results.

In the static limit, where the D -meson momentum is going to zero, one has the property

$$\lim_{p \rightarrow 0} [B_0(p) - B_1(p)] = 0, \quad (22)$$

which can be obtained from Eqs. (17,18). In this limit the Einstein relation between the thermal relaxation rate, γ , and diffusion coefficient, $B = B_0 = B_1$, is fulfilled and defined as

$$B = \gamma m_D T, \quad (23)$$

where $m_D = 1.87$ GeV is the mass of D -meson. In this work the Einstein relation is fully satisfied at lower temperatures, but starts to deviate slightly with increasing temperature. At the chemical freeze-out temperature, $T_{\text{ch}} = 170$ MeV, the deviation is of order of 25%.

The relaxation time, τ_R , which is defined by

$$\tau_R = \frac{1}{\gamma}, \quad (24)$$

for D -mesons in hadronic matter at the critical temperature, T_c , is approx. equal to 10 fm/ c . This value is in a good agreement with the corresponding value for c -quarks in QGP. Thus the "crossover" constrain is satisfied in our approach.

Finally, we calculate the spatial diffusion coefficient, D_x , which describes the broadening of the spatial distribution with time,

$$\langle \mathbf{x}^2(t) \rangle - \langle \mathbf{x}(t) \rangle^2 \simeq 6D_x t, \quad (25)$$

and it can be related to the thermal relaxation rate and diffusion coefficient through

$$D_x = \lim_{p \rightarrow 0} \frac{B}{m_D^2 \gamma^2}. \quad (26)$$

In Fig. 6 we present the results for the spatial diffusion coefficient calculated in our approach with (dash-dotted line) and without (solid line) the introduction of the effective chemical potentials to the hadronic cocktail in comparison to the results from Ref. [31] (dashed line), where the effective chemical potentials are not included. At the critical temperature there is a very smooth transition between our calculations for the hadron gas and the IQCD results taken from Ref. [53]. The difference between the results at higher temperatures shown by solid and dashed lines can be explained by the presence of the higher states in our hadronic cocktail.

V. THE NUCLEAR MODIFICATION FACTOR AND ELLIPTIC FLOW OF D -MESONS

The size of the transport coefficients in hadronic matter shows that the hadronic contributions should be included when evaluating the nuclear suppression factor and the elliptic flow of D -mesons as well as of single non-photon electrons.

We implement the transport coefficients calculated in the hadronic matter with the introduction of effective chemical potentials (Fig. 4) to the MC@sHQ model and calculate the nuclear modification factor, R_{AA} , and elliptic flow, v_2 , for two different scenarios:

1. *scenario I*: we use the transport coefficients, drag and diffusion coefficients, obtained from Eq. (20), however, in this case it is not evident that the asymptotic solution of the FP equation (8) is the thermal equilibrium distribution function.
2. *scenario II*: we employ the drag coefficient, obtained from Eq. (20), and assume, $B = B_0 = B_1$, calculated by Eq. (23). Thus we impose the Einstein relation which is valid only for small momenta. The Einstein relation ensures us that the asymptotic distribution function is the Boltzmann distribution function.

We consider both scenarios I and II to provide an idea of the theoretical systematic uncertainties of the FP approximation to the full Boltzmann equation.

In Fig. 7 we show the results for R_{AA} and v_2 of D -mesons and of single nonphoton electrons as a function of the transverse momentum. The comparison with the experimental data is presented, too. According to these results we can conclude that the D -meson rescattering in the hadronic gas is almost invisible for the R_{AA} because of the compensation between the extra cooling and extra radial flow, but shows a systematic increase of 1%-2% to the v_2 of D -mesons and of decay electrons. The results of

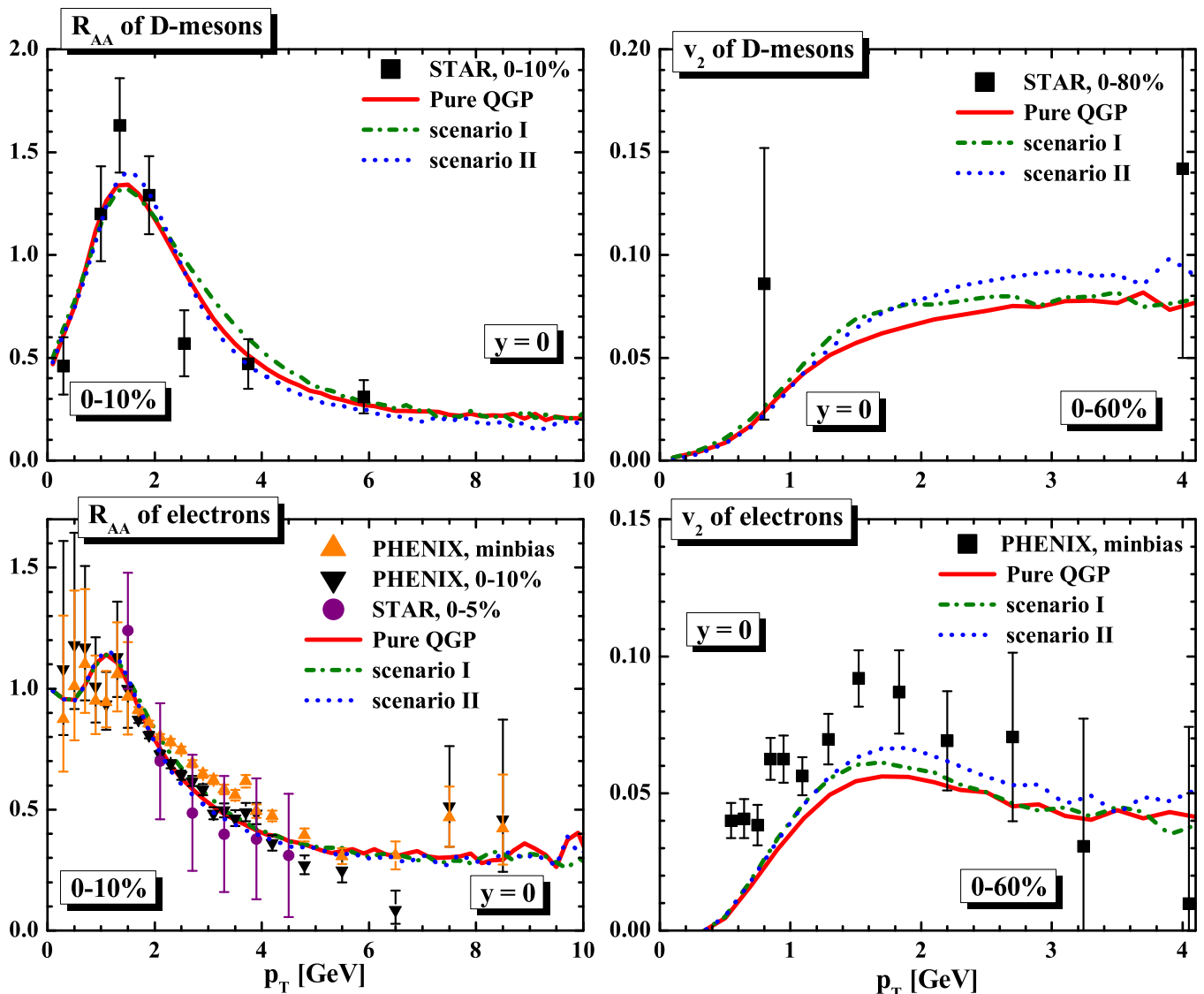


FIG. 7: The nuclear modification factor, R_{AA} , and elliptic flow, v_2 , of D -mesons and of single nonphotonic electrons originating from the decays of HF mesons for two scenarios as well as for pure QGP scenario in comparison to the experimental data from STAR and PHENIX experiments: R_{AA} of D -mesons - Ref. [8], v_2 of D -mesons - Ref. [9], R_{AA} and v_2 of decay electrons - Ref. [6, 7].

other groups [54, 55] also indicate the important role of the hadronic matter in the suppression and elliptic flow of HF mesons.

VI. THE D -MESON TRANSPORT COEFFICIENTS AT FAIR ENERGIES

In this section we construct the hadronic isentropic trajectories, i.e., with fixed specific entropy density, appropriate at future FAIR and NICA heavy-ion experiments. In particular, for FAIR physics, the beam energy will run from $\sqrt{s} = 5 - 40$ AGeV, which approximately corresponds to $s/\rho_B^{\text{net}} = 10 - 30$ [56]. We take three char-

acteristic values of $s/\rho_B^{\text{net}} = 10, 20, 30$ and show in Fig. 8 the results for the thermal relaxation rate (left panel) and the spatial diffusion coefficient (right panel) of D -meson for these trajectories as a function of temperature in comparison to the model estimates from Ref. [31]. We find that the D -meson thermal relaxation rate, γ , and the spatial diffusion coefficient, D_x , strongly depend on the isentropic trajectory. The impact of baryons to the transport coefficients becomes more important due to the large values for the baryon chemical potential corresponding to the isentropic trajectories, which are used. We remind that we use the same cross sections for D -meson rescattering with hadrons in the medium as in Ref. [31]. The difference between presented results is due to the

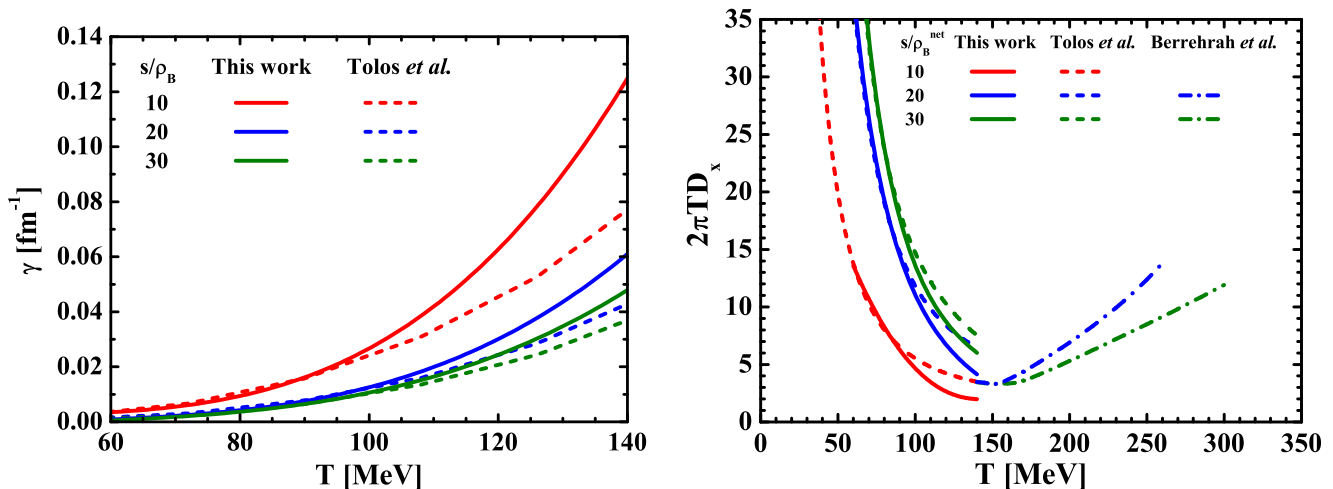


FIG. 8: The thermal relaxation rate (left panel) and the spatial diffusion coefficient (right panel) of D -meson for three different isentropic trajectories as a function of temperature in comparison to the model estimates from Ref. [31] (dashed lines). The results for the spatial diffusion coefficient of c -quarks propagating in the partonic medium obtained in Ref. [57] are shown by the dash-dotted lines.

presence of the higher states in our hadronic cocktail as they play a significant role at higher temperatures. Up to now, the approach in Ref. [24] was not extended to the finite chemical potentials. We therefore compare our results with the results for the spatial diffusion coefficient of c -quarks propagating in the partonic medium calculated in Ref. [57]. The comparison is presented in the right panel of Fig. 8. For the isentropic trajectory with $s/\rho_B^{\text{net}} = 20$ there is a perfect matching of results for D -mesons and c -quarks propagating through the hadronic and partonic matter, respectively.

VII. SUMMARY

Heavy mesons, created in ultrarelativistic heavy-ion collisions, are presently considered as a very good observable to improve our knowledge of the time evolution of the QGP, formed in these collisions. Being produced in hard collisions with no initial elliptic flow their thermalization time is considerably larger than the expansion time of the QGP. Therefore the final spectra of heavy mesons as well as their elliptic flow carry information on the interaction of the heavy quarks with the QGP partons. In order to obtain a quantitative evaluation of the modification of the heavy quark momentum distribution due to collisions with QGP particles the influence of hadronic rescattering of heavy mesons on the spectra has to be studied. Employing drag and diffusion coefficients based on the most recent calculations of the cross

section of D -mesons with the hadronic environment, we use the FP equation to determine the importance of the hadronic rescattering on the heavy meson spectra. We find that the influence on R_{AA} is negligible because of the compensation of the extra cooling and extra radial flow, whereas for the elliptic flow the influence is visible but small as compared to the elliptic flow the heavy quarks acquire during the expansion of the QGP.

We also extend our calculations to the finite chemical potentials, appropriate at future FAIR and NICA experiments, and show the D -meson spatial diffusion coefficient. We find that for the isentropic trajectory with $s/\rho_B^{\text{net}} = 20$ there is a perfect matching of our results with the results for c -quarks propagating in the partonic medium calculated in Ref. [57].

Acknowledgments

We thank E. L. Bratkovskaya, H. Berrehrah, D. Cabrera and H. van Hees for fruitful discussions. We also thank E. L. Bratkovskaya for providing us the code to simulate the hadron matter. This work was supported by the Project TOGETHER (Pays de la Loire) and I3-Hadronphysics II. V.O. acknowledges financial support from the HGS-HIRe Program. L.T. acknowledges support from the Ramon y Cajal Research Programme from Ministerio de Ciencia e Innovación and from Ministerio de Ciencia e Innovación under contracts FPA2010-16963 and FPA2013-43425-P.

[1] J. Adams *et al.* (STAR Collaboration), Nucl. Phys. A **757**, 102 (2005).

[2] K. Adcox *et al.* (PHENIX Collaboration), Nucl. Phys. A

- 757**, 184 (2005).
- [3] I. Arsene *et al.* (BRAHMS Collaboration), Nucl. Phys. A **757**, 1 (2005).
- [4] B. B. Back *et al.* (PHOBOS Collaboration), Nucl. Phys. A **757**, 28 (2005).
- [5] K. Aamodt *et al.* (ALICE Collaboration), Phys. Rev. Lett. **105**, 252302 (2010).
- [6] A. Adare *et al.* (PHENIX Collaboration), Phys. Rev. Lett. **98**, 172301 (2007).
- [7] B. Abelev *et al.* (STAR Collaboration), Phys. Rev. Lett. **98**, 192301 (2007).
- [8] X. Dong (STAR Collaboration), Nucl. Phys. A **904-905**, 19c (2013).
- [9] D. Tlusty (STAR Collaboration), Nucl. Phys. A **904-905**, 639c (2013).
- [10] B. Abelev *et al.* (ALICE Collaboration), J. High Energy Phys. 09 (2012) 112.
- [11] S. Sakai *et al.* (ALICE Collaboration), Nucl. Phys. A **904-905**, 661c (2013).
- [12] B. Abelev *et al.* (ALICE Collaboration), Phys. Rev. Lett. **111**, 102301 (2013).
- [13] B. Svetitsky, Phys. Rev. D **37**, 2484 (1988).
- [14] H. van Hees and R. Rapp, Phys. Rev. C **71**, 034907 (2005).
- [15] G. D. Moore and D. Teaney, Phys. Rev. C **71**, 064904 (2005).
- [16] M. G. Mustafa, Phys. Rev. C **72**, 014905 (2005).
- [17] P. B. Gossiaux, V. Guiho, and J. Aichelin, J. Phys. G **31**, S1079 (2005); J. Phys. G **32**, S359 (2006).
- [18] H. van Hees, V. Greco, and R. Rapp, Phys. Rev. C **73**, 034913 (2006).
- [19] C. M. Ko and W. Liu, Nucl. Phys. A **783**, 233 (2007).
- [20] Y. Akamatsu, T. Hatsuda, and T. Hirano, Phys. Rev. C **79**, 054907 (2009).
- [21] S. K. Das, Jan-e Alam, and P. Mohanty, Phys. Rev. C **82**, 014908 (2010).
- [22] W. M. Alberico, A. Beraudo, A. De Pace, A. Molinari, M. Monteno, M. Nardi, and F. Prino, Eur. Phys. J. C **71**, 1666 (2011).
- [23] S. Cao, G.-Y. Qin, and S. A. Bass, Phys. Rev. C **88**, 044907 (2013).
- [24] P. B. Gossiaux and J. Aichelin, Phys. Rev. C **78**, 014904 (2008).
- [25] P. B. Gossiaux, R. Bierkanndt, and J. Aichelin, Phys. Rev. C **79**, 044906 (2009).
- [26] M. Laine, J. High Energy Phys. 04 (2011) 124.
- [27] M. He, R. J. Fries, and R. Rapp, Phys. Lett. B **701**, 445 (2011).
- [28] S. Ghosh, S. K. Das, S. Sarkar, and Jan-e Alam, Phys. Rev. D **84**, 011503 (2011).
- [29] L. Abreu, D. Cabrera, F. J. Llanes-Estrada, and J. M. Torres-Rincon, Ann. Phys. **326**, 2737 (2011).
- [30] L. M. Abreu, D. Cabrera, and J. M. Torres-Rincon, Phys. Rev. D **87**, 034019 (2013).
- [31] L. Tolos and J. M. Torres-Rincon, Phys. Rev. D **88**, 074019 (2013).
- [32] J. M. Torres-Rincon, L. Tolos, and O. Romanets, Phys. Rev. D **89**, 074042 (2014).
- [33] M. He, R. J. Fries, and R. Rapp, Phys. Rev. C **86**, 014903 (2012).
- [34] S. K. Das, S. Ghosh, S. Sarkar, and Jan-e Alam, Phys. Rev. D **85**, 074017 (2012).
- [35] P. B. Gossiaux, J. Aichelin, T. Gousset, and V. Guiho, J. Phys. G **37**, 094019 (2010).
- [36] P. F. Kolb and U. Heinz, in *Quark-Gluon Plasma 3*, edited by R. C. Hwa *et al.* (World Scientific, Singapore, 2004), p. 634.
- [37] M. Cacciari, M. Greco, and P. Nason, J. High Energy Phys. 05 (1998) 007.
- [38] M. Cacciari, S. Frixione, and P. Nason, J. High Energy Phys. 03 (2001) 006.
- [39] M. Cacciari, S. Frixione, N. Houdeau, M. L. Mangano, P. Nason, and G. Ridolfi, J. High Energy Phys. 10 (2012) 137.
- [40] B. L. Combridge, Nucl. Phys. B **151**, 429 (1979).
- [41] Y. L. Dokshitzer, G. Marchesini, and B. R. Weber, Nucl. Phys. B **469**, 93 (1996).
- [42] A. Peshier, Phys. Rev. Lett. **97**, 212301 (2006).
- [43] S. Peigne and A. Peshier, Phys. Rev. D **77**, 114017 (2008).
- [44] A. C. Mattingly and P. M. Stevenson, Phys. Rev. D **49**, 437 (1994).
- [45] S. J. Brodsky, S. Menke, C. Merino, and J. Rathsman, Phys. Rev. D **67**, 055008 (2003).
- [46] E. Braaten and M. H. Thoma, Phys. Rev. D **44**, 1298 (1991).
- [47] E. Braaten and M. H. Thoma, Phys. Rev. D **44**, R2625 (1991).
- [48] M. Cacciari, P. Nason, and R. Vogt, Phys. Rev. Lett. **95**, 122001 (2005).
- [49] R. Rapp, Phys. Rev. C **66**, 017901 (2002).
- [50] E. L. Bratkovskaya, W. Cassing, C. Greiner, M. Effenger, U. Mosel, and A. Sibirtsev, Nucl. Phys. A **675**, 661 (2000).
- [51] P. F. Kolb and R. Rapp, Phys. Rev. C **67**, 044903 (2003).
- [52] Z. Lin, T. G. Di, and C. M. Ko, Nucl. Phys. A **689**, 965 (2001).
- [53] D. Banerjee, S. Datta, R. Gavai, and P. Majumdar, Phys. Rev. D **85**, 014510 (2012).
- [54] O. Linnyk, E. L. Bratkovskaya, and W. Cassing, Int. J. Mod. Phys. E **17**, 1367 (2008).
- [55] M. He, R. J. Fries, and R. Rapp, Phys. Rev. Lett. **110**, 112301 (2013).
- [56] L. V. Bravina *et al.*, Phys. Rev. C **78**, 014907 (2008).
- [57] H. Berrehrhah, P. B. Gossiaux, J. Aichelin, W. Cassing, J. M. Torres-Rincon, and E. Bratkovskaya, arXiv: 1406.5322 [hep-ph].